Chapter 9

Cellulose - Chitosan Nanocomposites - Evaluation of Physical, Mechanical and Biological Properties

Guillermo H. Riva, Joaquín García-Estrada, Brenda Vega, Fernando López-Dellamary, María E. Hérnandez and José A. Silva

Additional information is available at the end of the chapter

http://dx.doi.org/10.5772/61727

Abstract

This research describes the preparation of membranes with chitosan (CS) as the polymeric matrix and cellulose nanocrystals (CNC) as reinforcement. The aim was to evaluate their physical, mechanical and biological properties, and to determine their potential for biomedical use. Membranes were prepared via casting CNC suspensions in CS solution, at CNC concentrations of 0.5%, 1.0% and 2.0% (w/w) with pure chitosan as a reference. Analysis of membrane properties was performed using several techniques, such as ATR – FTIR, SEM, swelling test, maximum water absorption, dynamical mechanical analysis and *in vivo* (Winstar rats) biocompatibility and biodegradability assays for biological evaluation. Experimental results established that CNC reduced swelling rates and increased the maximum water absorption when CNC concentration was higher. Therefore, the presence of CNC in the matrix reduced Young's modulus by approximately 50% in comparison with pure chitosan. All formulations demonstrated biocompatibility and biodegradability values ranged between 4% and 21% in the 30 days after implantation. Based on these results, these membranes may be of use for biomedical applications.

Keywords: Cellulose nanocrystals, chitosan, biomedical, biocompatibility, nanocomposites

1. Introduction

1.1. Nanotechnology in actual context

The advances in nanotechnology for biomedical use are increasing and are at the forefront of scientific research. In recent years, hot spot areas such as drug transportation, tissue regener-

ation or nanomaterial development for cell-growth scaffolds have been constantly advancing. Biomaterials that are considered for biomedical applications must confirm to strict biological, physical and mechanical characteristics. Some biopolymers in particular, offer advantages in terms of sustainability and low environment impact compared to ceramics and metals. These attributes are the *biocompatibility* (an absence of inflammatory, cytotoxicity or invasive response in native cells, tissues or organs in vivo), *biodegradability* and *bioabsorbability* (the material and its by-products will degrade and/or be absorbed or safety eliminated from the body). More suitable properties may be the *degradation rate* (this rate must match the regeneration time of tissue in damaged zones, as well as transfer the mechanical efforts to new tissue in a timely manner), *porosity* (directly linked to mass transport and efficient tissue regeneration) and *surface morphology*. As drawbacks, the physical and mechanical properties of these materials make them less suitable than petroleum based plastics and other materials (metals, alloys and clays). As a consequence, reinforcement of the matrix is an option to counterbalance some of those drawbacks.

1.2. Biopolymers

1.2.1. Cellulose

Cellulose — the most abundant biopolymer on Earth — has an annual production of 7.5 x 10^{10} tons. This biopolymer is widely distributed in higher plants, sea animals (tunicates), and to a lesser degree in algae, fungi, bacteria, invertebrates, and is even found in protozoans such as *Dictyostelium discoideum*. In general, cellulose is a hard, fibrous, and water insoluble substance that plays an essential function in keeping the structure of cell walls in plants [1]. Cellulose can be found in its purest form in plants (i.e. cotton fibers). However, in wood, leaves and plant stalks, it is found mixed with other materials such as lignin and hemicelluloses. Cellulose nanofibers have the potential to be used in multiple ways, notably as a reinforcement material in the development of nanocomposites [2].

Thus, the preparation of biocompatible nanocomposites employing cellulose nanocrystals (CNC) as a reinforcement is a natural choice based on them being inert, biocompatible, biodegradable [3], and non-cytotoxic. They also contribute to the regeneration of damaged tissues or organs [4] and have mechanically desirable properties [5].

1.2.1.1. Types of processes used to obtain CNC

Cellulose nanocrystals (CNC) can be obtained by different techniques and processes:

a. Mechanical processes [6], i.e. using used bleached pulp of softwoods and hardwoods as a material raw to obtain nanocrystals from. The process begins with the soaking and grinding of fibers, followed by sieving and refining (for hardwoods this process is repeated several times). Finally, fibers are submitted to high pressure and homogenization processes (1000 Bar, 180 min), which are repeated until CNC is obtained. Energy consumption and Young's modulus (YM) are higher in hardwoods than softwoods. The tensile resistance in softwoods is better (75 MPa versus 63 MPa respectively).

http://dx.doi.org/10.5772/61727

b. Enzymatic processes [7], which have the advantage of simplifying the mechanical process of obtaining cellulose microfibers, mainly in the homogenization and disintegration stages. Acid hydrolysis was applied as a pre-treatment to the mechanical process. The sequence begins with refining and enzymatic treatment followed by a second refining and then homogenization. Endoglucanase was used as the enzyme and microfibers of 10–20 nm diameters were obtained.

c. Biological processes [8], a new method of obtaining nanocellulose using the Dutch elm disease fungus was established. The technique begins with the soaking and disintegrating of pulp in 2 liters of water, followed by 20 minutes in an autoclave with added sucrose and yeast to ensure feeding and growth. The fungus was left for 2–4 days at room temperature with mild stirring. Fibers were added to an autoclave to be washed again and the process finished with refining high speed cutting.

d. Chemical processes [1]. There are two basic methods for chemical modification: The first changes the surface energy characteristics of nanocrystals allowing an improvement in compatibility, especially when they are used with hydrophobic or non-polar matrices in nanocomposites, thereby obtaining a better dispersion in the matrix. The second method adds electric charges to the nanofibers (positive and negative) allowing a good dispersion. Acetylation of nanocrystals is an example of the first kind of modification [9], making their surfaces more hydrophobic. Kenaf fibers (*Hibiscus cannabius*) were modified using acetic anhydride before cellulose nanofibers were obtained from acetylated cellulose. This technique includes processes of disintegration, refining, cryorupture, and high pressure homogenization.

1.2.1.2. Nanocellulose for biomedical use

Nanocellulose has been called "biomaterials´ eyes" due to its potential for numerous applications in the biomedical field, including skin grafts to burn damage and wounds, growing of blood vessels, nerve reconstruction, brain membranes, and scaffolds in tissue engineering and bone reconstruction. Tissue engineering (TE) involves searching for new materials and artefacts to interact in positive ways with biological tissues. Furthermore, TI is seeking a primal artefact to cellular development *in vitro*, rearrangement and development of tissue when it will be implanted. The main attribute wanted in biopolymers with a potential biomedical use is a controllable and specific activity, to be used mainly in cellular scaffolds. Recently, many of these kinds of materials have been developed, having the required properties (physical/chemical and mechanical) dependent mostly on the final application (tissue regeneration, drug releasing, scaffolding, etc.). The success of scaffolds depends mainly on cellular adhesion and surface growth. The chemical surface of a biopolymer can cause the cellular response to interfere with the adhesion, proliferation, migration and cellular functionalization. The interaction in cell surface it's whole important in the graft, including its rejection. For the regeneration of tissues, three fundamental aspects are important: the cells, and the bearing and growing factors. The cells synthetize the matrix to new tissues, the bearing creates a suitable environment for cell development, and growing factors promote cell regeneration. Furthermore, regeneration must be promoted and if it is necessary, the new material must be absorbed

or biodegraded. Studies of the interactions of cell bearing are crucial for the feasibility of grafts. Different responses of cells can be observed from several materials, based on the ability of cells to distinguish and/or adapt to the surface of the material. This last factor is crucial, because it drives different responses such as cell proliferation, cell migration or feasibility. With issues regarding the skin, several laboratories have shown an interest in developing products that offer advantages such as the immediate mitigation of pain, close adhesion at wound surfaces and the reduction of infection rates. Nanocellulose has a large surface area that brings a better capability for water absorption and elasticity, these being the best characteristics for a recovering bandage, as microbial activity is stopped. Indeed, nanocellulose is very effective in reducing pain and promoting the granulation suitable for wound bandages. Another great advantage of nanocellulose consists in the capability to be built in any shape and size, making it ideal for covering extensive and difficult areas of the human body [10].

Hence, cellulose and CNC have been used in biomedicals. Past research has shown them to be ideal for tissue engineering, producing favorable results [3, 6]. CS membranes with nanoreinforcement must show a Young's modulus of 1,500—2,300 MPa to be suitable for biomedical use [11].

Furthermore, applications with excellent, proven results have been reported as follows [10]:

a. Pharmaceutical. Cellulose has excellent properties of compaction when it is mixed with other pharmaceutical excipients, forming dense matrices that make the administration of therapeutic drugs easy. Nanocellulose offers potential advantages as an excipient in drug release. Its large surface area and negative charge suggest that higher quantities of therapeutical drugs can be added to the surface of this material, showing the potential for a large quantity of charge and the optimal control of dosification. The proven biocompatibility of cellulose supports the use of nanocellulose for similar purposes. The hydroxide groups on the surface offer a site for surface modification to a broad range of chemical groups, using different methods. The surface modification can be used to tune the charge and drug release that are not normally linked with nanocellulose such as hydrophobic and non-ionized drugs.

b. Odontology. Nanocellulose can be used as biological barrier due to its porosity. This makes it ideal for use with infections, loss of fluids and it has an analgesic effect that allows therapeutic drugs be used easily and absorb the residual fluids during inflammatory stages, can be rejected in a controlled and painless way.

c. Ophthalmology [12]. Researchers explored the potential of nanocellulose as a scaffold and found it suitable for use in the development of tissue engineering for the cornea. They studied the growth of human stem cells in nanocellulose. The growth of corneal stem cells inside the scaffold was verified with a scanning laser microscope. The results suggested the potential of this biomaterial as a scaffold for tissue engineering of artificial corneas.

d. Vascular surgery [13]. Researchers studied artificial vascular implants of nanocellulose in two cases: The first was a microsurgery study, where nanocellulose implants were used as an artificial part of the carotid artery of rats for a year. These results showed the incorporation of nanocellulose under the formation of tissues and internal growth of

http://dx.doi.org/10.5772/61727

active fibroblasts over a long period. In a second study, the implants were used to replace the carotid artery of pigs. After three months, the implants were retired and analyzed at both macro and microscopic levels. Seven implants (87.5%) were found in use and just one of them was blocked. This data showed that the innovative techniques of nanocellulose engineering have allowed the production of stable vascular conduits and confirmed the very notable achievement of the use of tissues for blood vessels in vivo as a part of cardiovascular programs.

e. Reconstructive / aesthetic surgery [14] Ideal for nasal reconstruction. The response of tissue in the presence of nanocellulose in nose bone was evaluated. In the study, 22 rabbits were used and in 20 of them a cellulose film was added to the nasal dorsum, with the remaining two acting as a control. After three and six months, the new bone was extracted for histopathology studies. Parameters such as blocking of blood flow, inflammation intensity and inflammation by the presence of purulent liquids were found to be stable, probably due to the surgical process itself rather than the presence of cellulose. For the other parameters, the statistical response was not significant. The nanocellulose coverage showed good compatibility and remained unchanged over time, making this material an excellent option for rebuilding new bone.

1.2.2. Chitosan

Chitosan (CS) is a biomaterial of proven use in the biomedical field due its biocompatibility, biodegradability and antibacterial activity, making it ideal for drug transportation, tissue engineering, wound healing, and antibacterial uses [15]. Furthermore, chitosan is bioactive and nontoxic. This biopolymer has a wide range of uses such as substance separation due to its barrier property and sensors, as well as food packing. Other authors describe the preparation of bionanocomposites using chitosan and different nanoreinforcements with the goal of obtaining a better mechanical performance, as well as the barrier properties and sensing detectors [16]. Chitosan is commonly amorphous and can be processed in flexible films. It is bioactive, non-toxic, and suited to biomedical applications such as pharmaceutical products like films, pearls or spheres, and gels, powders, etc. Previous works in cellulose-chitosan nanocomposites showed good results in physical, mechanical and biological tests [17, 18].

Chitosan can form flexible, clean and hard films [19] with a good oxygen barrier [20]. Furthermore, it can be used as packing material, mainly as a covering and edible film [21] extending the average life of foods [22, 23]. Chitosan can also form a semipermeable covering to modify the inner atmosphere, thereby reducing the transpiration rate of the product in the packaging [24]. Despite good results with respect to their mechanical properties, chitosan films can be brittle, making it necessary to use plasticizers to increase their flexibility [25]. Plasticizers such as glycerol can improve the processability, as well as the mechanical properties of chitosan [26]. In another study, researchers reported a concentration of 20% (w/w) of glycerol as the appropriate concentration to improve the flexibility of chitosan films [27]. To prevent this drawback of rigidity and brittleness of chitosan, the addition of reinforcement has showed to be useful in enhancing its mechanical, thermal and barrier properties. When the particles are smaller, the interaction with the matrix is better [28], with the low cost a sign of efficiency [29].

Fillers on a nanometric scale (called nanoparticles or nanoreinforcements) with good dispersion drive an interface matrix / filler, changing the molecular mobility, relaxation behavior and thermal and mechanical properties of the material [30].

A positive result in the elaboration of chitosan – CNC nanocomposites was obtained, using electrospinning for fibers of a derivative of chitosan / cellulose in an ionic liquid (IL). The chitosan / cellulose composite were electrospun in the ethanol co-solvent, using the IL to dissolve the chitosan and cellulose at the same time. Furthermore, the IL was capable of building fibers of pure chitosan / cellulose composite after the IL was removed by the ethanol. The fibers of this composite were manufactured as a three-dimensional shape, offering antibacterial activity to treat burns, bedsores and skin ulcers [31].

Nanofibers were obtained from chitosan and cellulose, with chitin used as a reinforcement material at different concentrations (from 1.25% to 5.0% w/w). This allowed the optimizing of the process conditions to obtain homogeneous and porous nanofibers. This material has a potential for use in wound bandages and skin burns [32].

Layer-by-Layer technique (LbL) is a technique to elaborate nanocomposites of chitosan and cellulose whiskers. The interactions between amine groups (chitosan) and sulfate groups (cellulose whiskers) ensure the linkages between matrix and nanoreinforcement to elaborate the films. The average thickness of each bi-layer (whiskers / chitosan) was 7 nm and each film was formed by 30 bi-layers. These materials have a wide range of uses such as packaging and biomedicals [15].

Chitosan films used for cell scaffolding in the regeneration of the tympanic membrane (type I experimental tympanoplasty) were elaborated. These films were grafted in New Zealand rabbits with successful results of tympanic tissue regeneration [33].

2. Objective

Demonstrate that CNC can improve the mechanical and physical properties of a chitosan matrix. Furthermore, determine the biocompatibility and biodegradability of CS and CNC nanocomposites via biological tests and then based on the results obtained, determine a potential use of these nanocomposites in the biomedical area.

3. Experimental

3.1. Materials

Materials used for this study were Biomedical Grade chitosan from Sigma Aldrich (Deacetylation grade 75–85%), acetic acid, alpha cellulose (Neucel Cellulose Ltd.), male laboratory rats (Wistar), cellulose acetate membranes for dialysis, vacuum oven, high resolution microscopy, dynamical-mechanical and chemical analysis. The formulations employed in this research are presented in Table 1.

http://dx.doi.org/10.5772/61727

Material	Reinforcement	Formulation (w/w)
CS	CNC	Pure CS
		CS + CNC (0.5%)
		CS + CNC (1.0%)
		CS + CNC (2.0%)

Table 1. Formulations of CS + CNC films

3.2. Methodology

- Preparation of CNC

Alpha cellulose was ground and mixed with sulfuric acid (64% concentration) for one hour under constant stirring and at a controlled temperature (approximately 50° C in a warm bath). After that, the liquor was added to deionized water, cooled at 8° C 1:10 (v/v) to stop the reaction. The liquor was centrifuged at 4000 RPM for 5 minutes, separating the liquor into two phases: solid (cellulose gel in the bottom of recipient) and liquid (with acid remainders). The liquid phase was disposed of and deionized water was added to the recipient to remove excess acid from the gel (containing CNC), prior to centrifugations (three in total). The washed gel was put in dialysis membranes in deionized water under stirring until it reached a pH of 5. After that, the CNC were submitted to ultrasound treatment for 2 minutes and finally vacuum filtered using 0.45 micron Wharton paper, and kept cooled.

- Chitosan – CNC films elaboration

Chitosan (4 g) was dissolved in acetic acid at 2% (v/v) per each formulation, under constant stirring for 2 hours. Next, CNC in different concentrations were added (0.5%, 1.0% and 2.0%) and then stirred for two more hours. The substance was cast on Petri plates affording a concentration of 0.4 mL/cm^2 to obtain the same quantity of nanocomposite on the plates. The plates were then put into a vacuum oven (28°C–70 MPa) for 96 hours. After drying, NaOH (1.0 N) was added to the Petri dishes to precipitate the films and then the CS + CNC films were washed with deionized water until they reached a pH of 7. Finally, films were dried at room temperature for 48 hours. The thickness of films was measured with a micrometer and dimensioned for physical and mechanical testing.

- Physical evaluation

When performing swelling tests, modifications in the dimensions of specimens were made to evaluate swelling changes over time. The dry weight (W_i) of each specimen was taken and then films of each formulation were put in deionized water to control the weight each minute until a constant value was achieved [34]. For maximum water retention (MWR), the dry weight (W_i) of each specimen (8 per formulation) was taken and it was then added to deionized water. Weights were controlled at 30, 60, and 120 minutes, and then 24 hours, before the final weight was obtained (W_f) [34]. Finally, the MWR was determined by the following formula:

$$\mathrm{MWR}\ (\%) = (W_f - W_i) \,/\, (W_i) \times 100$$

- Mechanical evaluation

Dynamical mechanical analysis was used in static mode to evaluate Young's modulus for all formulations, with the stress-strain test operating in the controlled force mode. Typical testing conditions were 0.1 N preload, 1 N/min ramp and a gauge length of ca. 10 mm. Strips of 0.075 mm x 5 mm x 20 mm were used. The temperature range was 37.05 ± 0.05°C and the moisture content was 98%, determined by a TA Instruments DMA 800 used in wet conditions.

- Biological evaluation

The best way to test our material was in living specimens. Biocompatibility and biodegradability tests were carried out. For these, the dry weight (W_i) of films was controlled. The biological subjects for testing were 16 Lab rats (of the Wistar breed). The animals were submitted to a surgical procedure involving grafting two portions of films for each formulation (4 rats per formulation). Each animal had two sub-cutaneous cuts (in the middle of back, on the right side for biocompatibility and on the left side for biodegradability). Every three days, the rats were controlled to prevent any infection or adverse reaction to the nanomaterial. Specimens were euthanized 30 days after surgery and the two portions of membrane were retired, lyophilized and controlled for dry weight (W_f) in order to obtain the biodegradability value:

Biodegradability (%) = $(W_i - W_f) / (W_i) \times 100$

Biocompatibility was proved by SEM images at the moment the grafts were retired, the mortality rate of specimens and the non-presence of encapsulation, fibrillation or any rotten portion of membrane after 30 days.

- Characterization of nanocomposites

To characterize the morphology of films, the response and the different levels of biocompatibility and biodegradability, a JEOL JM 6300 with a double gold layer to avoid the electrical charge of the sample was used. The magnification was from around 500x up to 35,000x and the voltage employed was between 7kV and 20kV.

- IR spectroscopy

This technique was used to determine changes in functional groups of nanocomposite as a consequence of the presence of CNC in the chitosan matrix, or previous chemical treatment. Portions of thin films of all formulations were analyzed in an IP Spectrometer in transmittance mode (4,000 to 500 cm^{-1}). Other parameters were: 16 scans per spectrum, ATR mode and a resolution of 0.4 cm^{-1}. A Perkin Elmer Spectrum GX FT-IR System was used.

4. Results

4.1. CNC + chitosan films

The films obtained from the combination of chitosan and CNC showed a transparent aspect with a slight yellow color. Transparence in the films suggests a good distribution of CNC in the CS matrix. At the same time, the slight yellow color is due to the natural presence of

resolution of 0.4 cm^{-1}. A Perkin Elmer Spectrum GX FT-IR System was used.

3. Results

http://dx.doi.org/10.5772/61727

3.1 CNC + chitosan films

The films obtained from the combination of chitosan and CNC showed a transparent aspect with a slight yellow color. Transparence in the films suggests a good distribution of CNC in the CS matrix. At the same time, the slight yellow color is due to the natural presence of impurities in this biopolymer [35]. The average thickness of films was 30 microns and the surface was smooth. Visible CNC agglomerates and dark points were absent from these films as can be seen in Figure 1.

These characteristics in all formulations of pure CS and CS + CNC were the same, and accorded with findings of other authors [19, 21, 35, 36]. Even with CNC concentrations over 20% (w/w), transparent films were reported, although with CNC concentrations over 60% the films showed a translucent appearance (a greyish color) and a rigid but brittle consistency [35]. Chitosan films and polyethylene oxide (PEO) employing electrospinning produced good results in transparence and homogeneity [32].

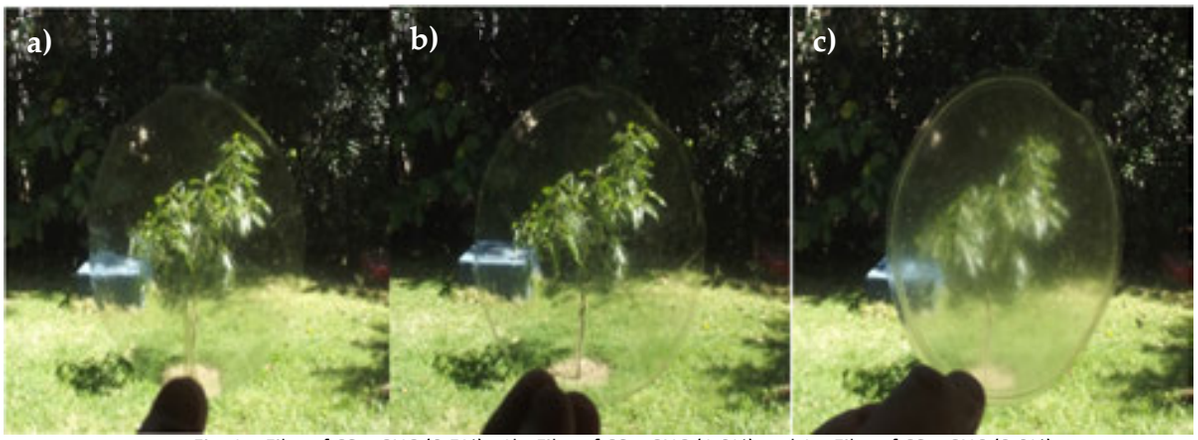

Fig. 1a. Film of CS + CNC (0.5%). 1b. Film of CS + CNC (1.0%) and 1c. Film of CS + CNC (2.0%)

Figure 1. a. Film of CS + CNC (0.5%). b. Film of CS + CNC (1.0%) and c. Film of CS + CNC (2.0%)

3.2 Morphology of CS + CNC films

4.2. Morphology of CS + CNC films

SEM images showed a good dispersion of CNC in the nanocomposites due to the affinity between the SEM images showed a good dispersion of CNC in the nanocomposites due to the affinity between the nanoreinforcement and the matrix (having similar chemical structure and hydrophilic nature), as well as a good interaction of negative charges of the sulfate groups of CNC with the amine groups of CS [35]. The presence of nanoparticles was observed in different formulations of nanocomposites, as can be seen in Figure 2. These bundles formed by several tens of CNC, with dimensions of between 150–200 nm up to 500 nm on average, and in some cases up to 1 or 2 microns, mainly in CS + CNC (2.0%). The phenomenon was common when the CNC concentration was higher (over 5% and 10%) and even when working with concentrations of 5% and 10% it was possible to see white punctuations in the matrix surface via SEM images, seen in the cross section of CNC [36]. Another possible phenomenon linked to a higher concentration of CNC in the matrix, is the formation of a polyelectrolyte macroion complex between CS and CNC. The size of these complexes could reach several microns in length. These particles are formed by CNC and surrounded by CS chains. The shape of these complexes depends on the quantity of NH_2 in CS. When the concentration of NH_2 is high, the shape of the complex tends to be spherical [37]. These particles could have potential in biomedicals for drug transportation and controlled release due to the charges on cellulose and the linkage that can be achieved with other substances and active composites.

CNC and surrounded by CS chains. The shape of these complexes depends on the quantity of NH_2 in CS. When the concentration of NH_2 is high, the shape of the complex tends to be spherical [37]. These particles could have potential in biomedicals for drug transportation and controlled release due to the charges on cellulose and the linkage that can be achieved with other substances and active composites.

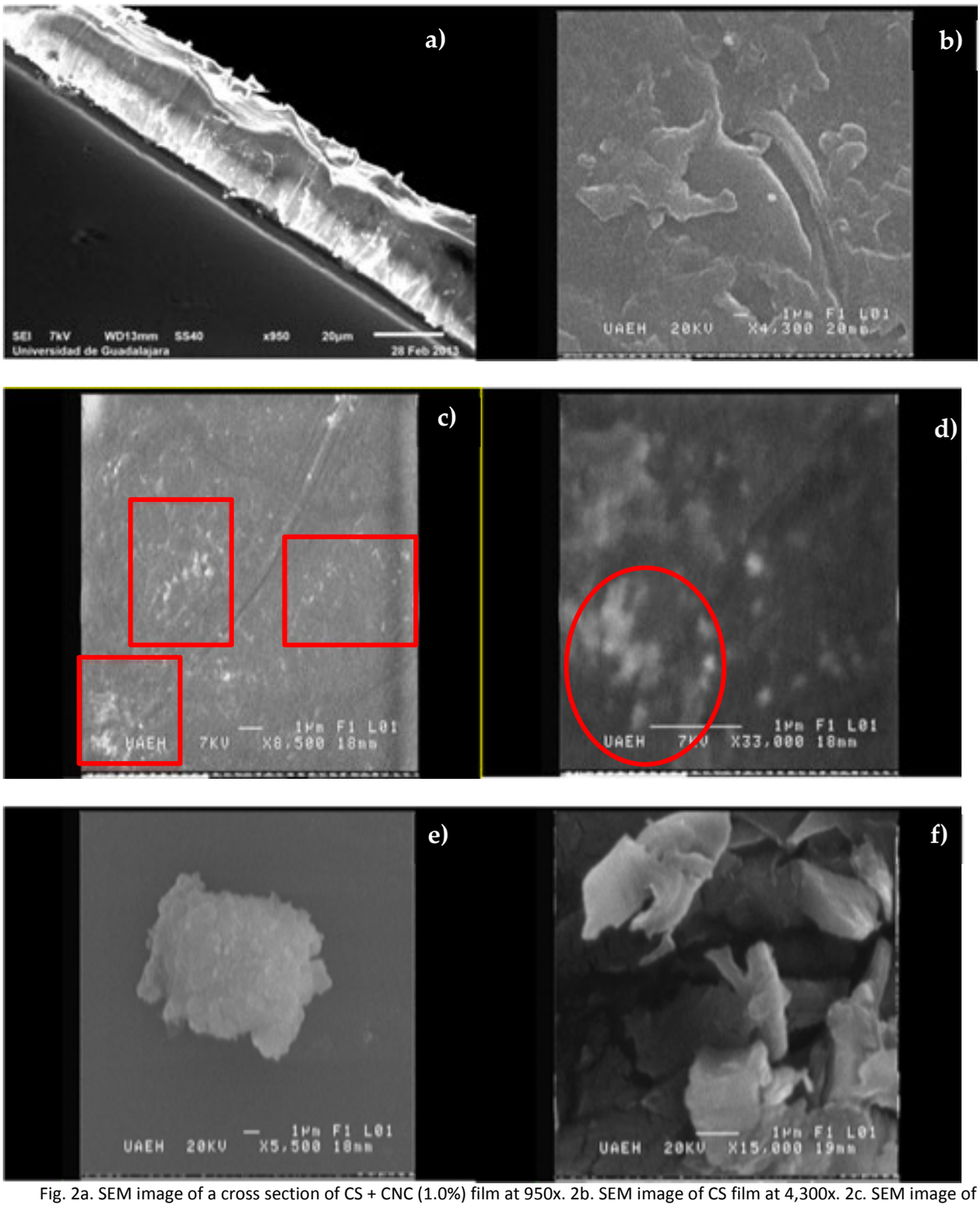

Fig. 2a. SEM image of a cross section of CS + CNC (1.0%) film at 950x. 2b. SEM image of CS film at 4,300x. 2c. SEM image of clusters of CS + CNC (0.5%) film at 8,500x (circled in red). 2d. SEM image of clusters of CS + CNC (0.5%) at 35,000x (circled in red). 2e CS – CNC (2.0%) macroion at 5,500x and 2f. CS + CNC (2.0%) at 15,000x.

Figure 2. a SEM image of a cross section of CS + CNC (1.0%) film at 950x. b. SEM image of CS film at 4,300x. c. SEM image of clusters of CS + CNC (0.5%) film at 8,500x (circled in red), d. SEM image of clusters of CS + CNC (0.5%) at 35,000x (circled in red). e CS – CNC (2.0%) macroion at 5,500x and 2f. CS + CNC (2.0%) at 15,000x.

3.3 Physical Properties

Swelling capability is presented in Figure 3. Swelling capability showed an evident change with the presence of CNC in the matrix. For water swelling, pure CS films showed saturation times of 3–4 minutes. With formulations of CS + CNC (0.5%) saturation times reduced to 1–2 minutes, while for formulations with CNC of 1% and 2%, the saturation time was 1 minute. These results show that CNC allow water entrance between CS chains as an unstructuring element, making the material more hydrophilic. This

http://dx.doi.org/10.5772/61727

CNC and surrounded by CS chains. The shape of these complexes depends on the quantity of NH_2 in CS. When the concentration of NH_2 is high, the shape of the complex tends to be spherical [37]. These particles could have potential in biomedicals for drug transportation and controlled release due to the charges on cellulose and the linkage that can be achieved with other substances and active composites.

4.3. Physical properties

Fig. 2a. SEM image of a cross section of CS + CNC (1.0%) film at 950x. 2b. SEM image of CS film at 4,300x. 2c. SEM image of clusters of CS + CNC (0.5%) film at 5,500x (model in red). 2d. SEM image of cross section of CS + CNC (0.5%) at 35,000x (deformed zone). 2e. CNC (2.0%) macrojon at 5,500x and 2f. CS + CNC (2.0%) at 15,000x.

Swelling capability is presented in Figure 3. Swelling capability showed an evident change with the presence of CNC in the matrix. For water swelling, pure CS films showed saturation times of 3–4 minutes. With formulations of CS + CNC (0.5%) saturation times reduced to 1–2 minutes, while for formulations with CNC of 1% and 2%, the saturation time was 1 minute. These results show that CNC allow water entrance between CS chains as an unstructuring element, making the material more hydrophilic. This behavior was opposite to that observed in another study, which used higher concentrations of CNC (from 5% up to 60%) making the CS films less permeable, thereby reducing the swelling capability significantly [35, 36, 38]. The maximum water retention (MWR) showed a similar response with the presence of CNC, as presented in Table 2.

3.3 Physical Properties

Swelling capability is presented in Figure 3. Swelling capability showed an evident change with the presence of CNC in the matrix. For water swelling, pure CS films showed saturation times of 3–4 minutes. With formulations of CS + CNC (0.5%) saturation times reduced to 1–2 minutes, while for formulations with CNC of 1% and 2%, the saturation time was 1 minute. These results show that CNC allow water entrance between CS chains as an unstructuring element, making the material more hydrophilic. This behavior was opposite to that observed in another study, which used higher concentrations of CNC (from 5% up to 60%) making the CS films less permeable, thereby reducing the swelling capability significantly [35, 36, 38]. The maximum water retention (MWR) showed a similar response with the presence of CNC, as presented in Table 2.

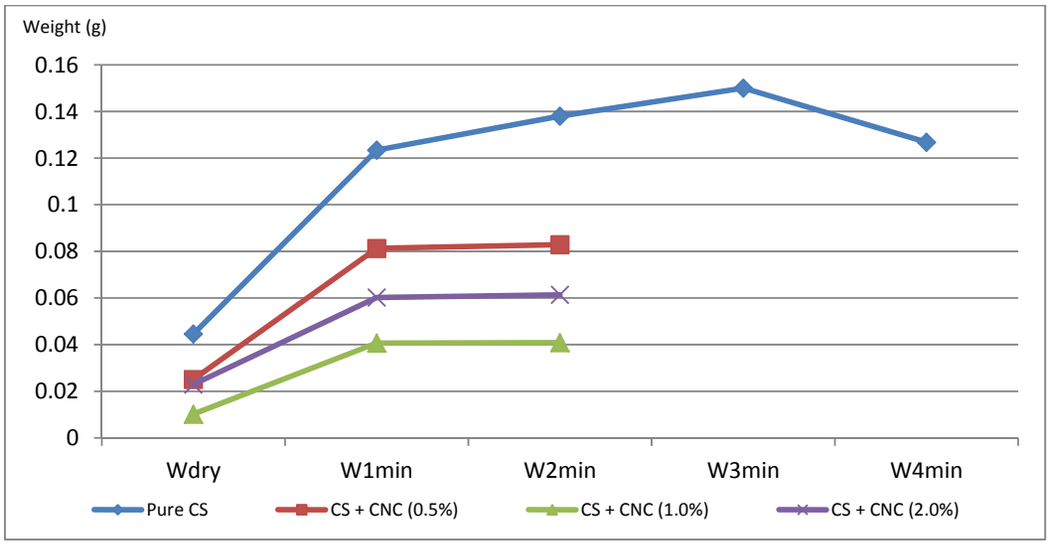

Fig. 3 Swelling capability for CS + CNC nanocomposites

Figure 3. Swelling capability for CS + CNC nanocomposites

Table 2 Values of MWR for CS + CNC nanocomposites

Formulation	Variation in time W30min	Variation in time W120min	Variation in time W24h
Pure CS	189.72	198.86	187.49
CS + CNC (0.5%)	237.68	222.67	226.64
CS + CNC (1.0%)	346.52	277.79	258.18
CS + CNC (2.0%)	234.68	236.70	214.65

Formulation	W30min	W120min	W24h
Pure CS	189.72	198.86	187.49
CS + CNC (0.5%)	237.68	222.67	226.64
CS + CNC (1.0%)	346.52	277.79	258.18
CS + CNC (2.0%)	234.68	236.70	214.65

Table 2. Values of MWR for CS + CNC nanocomposites

For pure CS films, the MWR was 187% of its own weight in water, while CS + CNC (0.5%) films obtained values of 226%, CS + CNC (1.0%) values of 258% and CS + CNC (2.0%) values of 214%, as can be seen in Figure 4. In these cases, the low concentrations of CNC improve the water

retention properties of films in comparison with results of other authors [15, 35] which showed a remarkable reduction in the physical properties of CS + CNC films, using concentrations from 5% up to 60%. This phenomenon can be explained by the affinity of CNC to the water, due their hydrophilic nature (and O–H linkages). Another reason is the plasticizing effect of CNC at low concentrations of CS matrix, contributing to the unstructuring effect in CS chains allowing the passage of water inside the polymer. This effect makes the film more flexible, facilitating the entry of water into the polymer chains. A similar effect was reported when adding different concentrations of glycerol (from 2% to 6%), used as a plasticizer in starch films with CS covering. Even at the highest CS concentration, the presence of glycerol increased this parameter, with values from 71.8% to 125.4% in comparison with pure CS (35.7% to 74.8%) [21].

CS covering. Even at the highest CS concentration, the presence of glycerol increased this parameter, with values from 71.8% to 125.4% in comparison with pure CS (35.7% to 74.8%) [21].

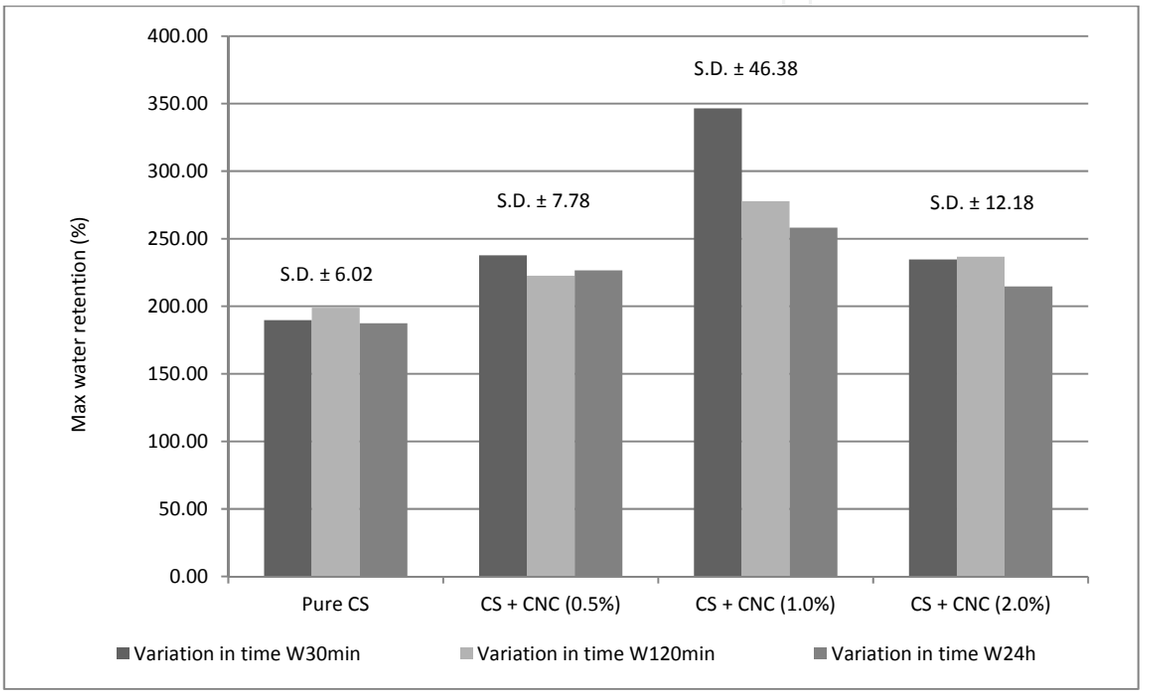

Fig. 4 Values (%) of maximum water retention for pure CS and CS + CNC films

Figure 4. Values (%) of maximum water retention for pure CS and CS + CNC films

3.4 Mechanical properties

4.4. Mechanical properties

The values obtained from formulations with CNC suggest that these modified the mechanical properties in comparison with pure CS. Young's modulus (YM) reached by pure CS was 2,916 ± 933 MPa, similar to that observed in another study [35], while for formulations with CNC the values were CS + CNC (0.5%) 1,575 ± 82 MPa, CS + CNC (1.0%) 1690 ± 433 MPa and for CS + CNC (2.0%) the value was 1657 ± 4 MPa, as can be seen in Figure 5. There was a large variation in the results for YM in pure CS, with values from 1,080 MPa up to 2,852 MPa. The average for pure CS ranged between 2,300 and 2,500 MPa. This variation is because the matrix polymer has crystalline and amorphous zones, which will exhibit different resistances (high and low values). Furthermore, residual efforts stored in films as a consequence of some conditions in their elaboration process (casting solution), appears in the first stages of assay, when the machine break these efforts first before apply all the force in the film in a homogeneous way.

The values obtained from formulations with CNC suggest that these modified the mechanical properties in comparison with pure CS. Young's modulus (YM) reached by pure CS was 2,916 ± 933 MPa, similar to that observed in another study [35], while for formulations with CNC the values were CS + CNC (0.5%) 1,575 ± 82 MPa, CS + CNC (1.0%) 1690 ± 433 MPa and for CS + CNC (2.0%) the value was 1657 ± 4 MPa, as can be seen in Figure 5. There was a large variation in the results for YM in pure CS, with values from 1,080 MPa up to 2,852 MPa. The average for pure CS ranged between 2,300 and 2,500 MPa. This variation is because the matrix polymer has crystalline and amorphous zones, which will exhibit different resistances (high and low values). Furthermore, residual efforts stored in films as a consequence of some conditions in their elaboration process (casting solution), appears in the first stages of assay, when the machine break these efforts first before apply all the force in the film in a homogeneous way.

Some explanations for the decrease of Young's Modulus in the films with GNC suggest the cause as the formation of aggregates and CS–CNC complexes due to the agglomeration of nanoparticles in one single place, generating stresses around them and becoming a potential weak point in the film. It could be deduced that CNC acted as a plasticizer of the matrix, making it less rigid. However, CS + CNC formulations showed values lower than those obtained for pure CS. However, these values were less variable than pure CS values and a further detail was observed: CNC aggregation didn't contribute to the deformation or rupture of films.

Another possible cause of the observed decrease in YM could be the low concentrations of CNC employed in this study (0.5%, 1.0% and 2.0%) in comparison with other studies that used concentrations above 5%,

http://dx.doi.org/10.5772/61727

The graphs showed an inflexion point in effort–strain curves. This phenomenon was present in some films of CS + CNC (1.0%) and CS + CNC (2.0%).

Some explanations for the decrease of Young's Modulus in the films with CNC suggest the cause as the formation of aggregates and CS–CNC complexes due to the agglomeration of nanoparticles in one single place, generating stresses around them and becoming a potential weak point in the film. It could be deduced that CNC acted as a plasticizer of the matrix, making it less rigid. However, CS + CNC formulations showed values lower than those obtained for pure CS. However, these values were less variable than pure CS values and a further detail was observed: CNC aggregation didn't contribute to the deformation or rupture of films.

Another possible cause of the observed decrease in YM could be the low concentrations of CNC employed in this study (0.5%, 1.0% and 2.0%) in comparison with other studies that used concentrations above 5%, 10% until 60% [15, 35] that saw improvements in YM of 78% to 150% and 230% to 320% respectively. The decrease in YM must be understood as a loss of stiffness, making a more flexible material, but with low strain values (1–2%). This last can be improved if plasticizers (i.e. glycerol) are included in the formulations. The values obtained are similar with CS films with chitin concentrations of 2.7% to 37.5%, having values from 1,622 ± 377 MPa to 2,318 ±619 MPa respectively [11]. Based on these values, a potential use of these films could be in healing and wound recovery, as well as scar prevention.

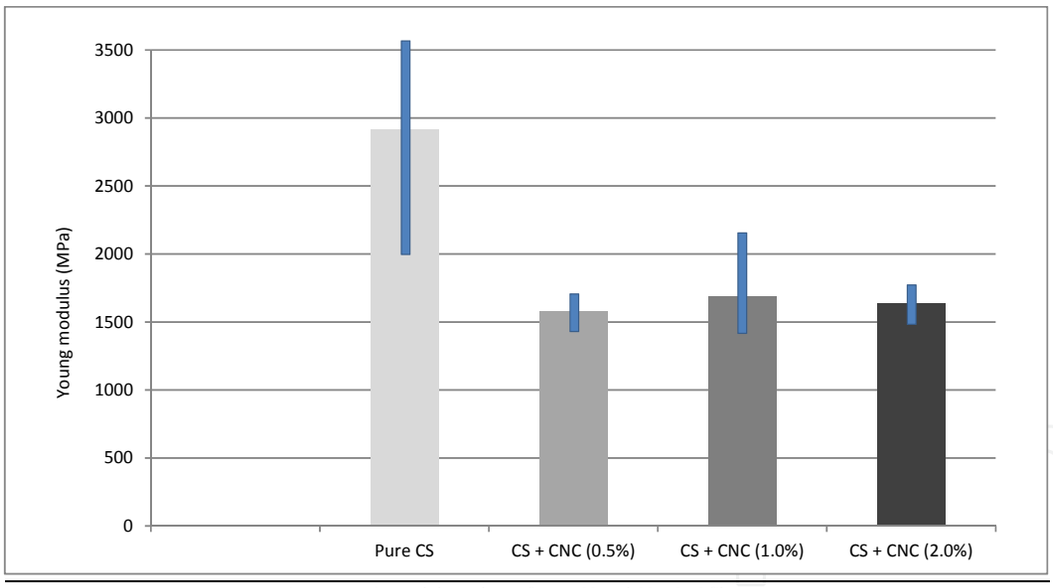

Fig. 5 Young's Modulus values of pure CS and CS + CNC films

Figure 5. Young's Modulus values of pure CS and CS + CNC films

3.5 IR Spectroscopy of CS + CNC films

As can be seen in Figure 6, for pure CS the IR spectrum showed bands at 3,360 and 3,265 cm^{-1} typical of O–H and N–H bonds respectively. The band at 2,870 cm^{-1} corresponds to C–H bonds and the signal at 1,650 cm^{-1} is commonly seen with type I amides and C=O bonds linked to acetyl and amine groups and 1,560 cm^{-1} corresponds to amide groups (N–H). Bands of 1,420 and 1,375 cm^{-1} correspond to residual CH_3N– racetyl glucosamine and $-CH_2$ groups respectively. Finally, bands of 1,060 and 1,030 cm^{-1} confirm the presence of C–O bonds.

Regarding nanocomposites, formulations of CS + CNC of 0.5%, 1.0% and 2.0% didn't show variations in their spectrums when compared with a pure CS spectrum, as shown in Figure 7. This is due to the similarity between cellulose and chitosan in terms of their chemical structure. For that reason, the bands for both polysaccharides are the same, except for the presence of an amine group with chitosan [15]. Another cause is the low concentration of CNC, which could be undetected by FTIR. A similar phenomenon has been observed in chitin, chitosan and glycerol nanocomposites [38].

4.5. IR Spectroscopy of CS + CNC films

As can be seen in Figure 6, for pure CS the IR spectrum showed bands at 3,360 and 3,265 cm^{-1} typical of O–H and N–H bonds respectively. The band at 2,870 cm^{-1} corresponds to C–H bonds and the signal at 1,650 cm^{-1} is commonly seen with type I amides and C=O bonds linked to acetyl and amine groups, and 1,560 cm^{-1} corresponds to amide groups (N–H). Bands of 1,420

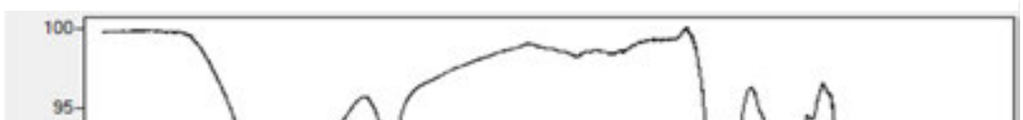

and 1,375 cm^{-1} correspond to residual CH_3N–acetyl glucosamine and $–CH_2$ groups respectively. Finally, bands of 1,060 and 1,030 cm^{-1} confirm the presence of C–O bonds.

Regarding nanocomposites, formulations of CS + CNC of 0.5%, 1.0% and 2.0% didn't show variations in their spectrums when compared with a pure CS spectrum, as shown in Figure 7. This is due to the similarity between cellulose and chitosan in terms of their chemical structure. For that reason, the bands for both polysaccharides are the same, except for the presence of an amine group with chitosan [15]. Another cause is the low concentration of CNC, which could be undetected by FTIR. A similar phenomenon has been observed in chitin, chitosan and glycerol nanocomposites [38].

Regarding nanocomposites, formulations of CS + CNC of 0.5%, 1.0% and 2.0% didn't show variations in their spectrums when compared with a pure CS spectrum, as shown in Figure 7. This is due to the similarity between cellulose and chitosan in terms of their chemical structure. For that reason, the bands for both polysaccharides are the same, except for the presence of an amine group with chitosan [15]. Another cause is the low concentration of CNC, which could be undetected by FTIR. A similar phenomenon has been observed in chitin, chitosan and glycerol nanocomposites [38].

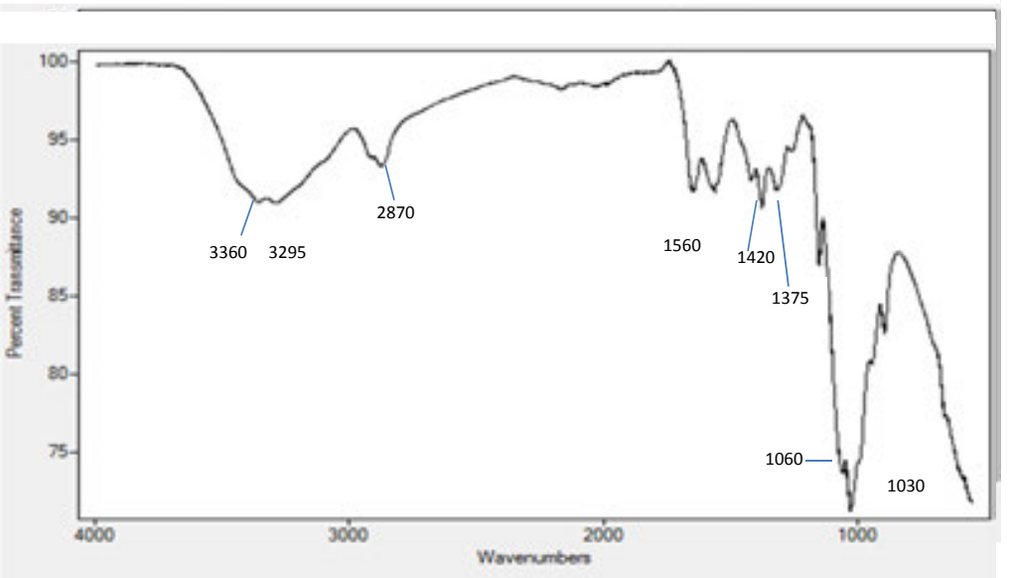

Fig. 6 IR spectrum of pure CS film

Figure 6. IR spectrum of pure CS film

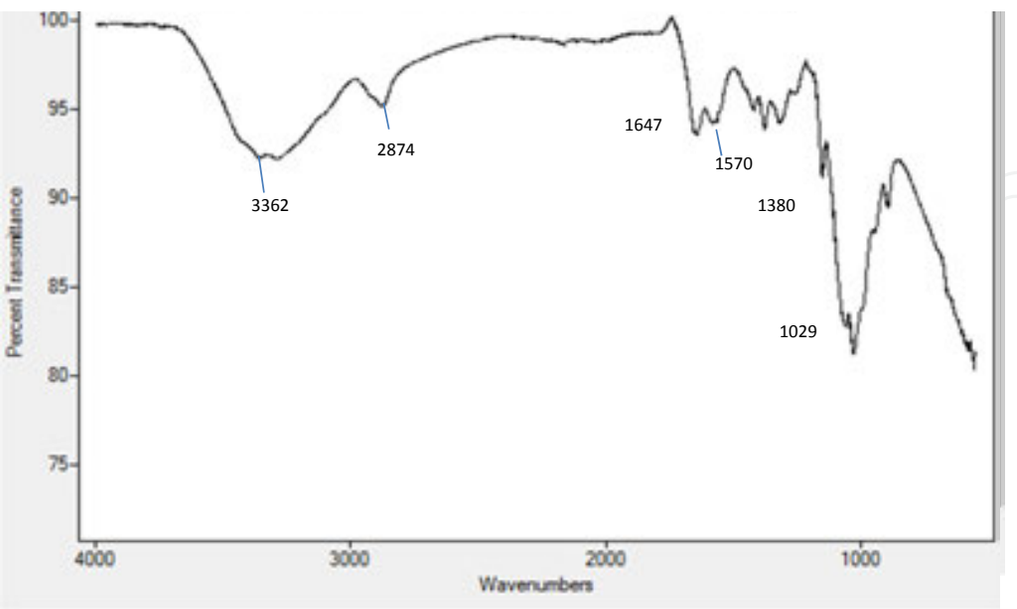

Fig. 7 IR spectrum of CS + CNC (2.0%) film

Figure 7. IR spectrum of CS + CNC (2.0%) film

3.6 Biological Testing

3.6 Biological Testing

Biological results showed 100% biocompatibility for all formulations in 16 rats. After 30 days, the specimens had not shown an adverse reaction, septicemia or death in the presence of CNC. At the point

Biological results showed 100% biocompatibility for all formulations in 16 rats. After 30 days, the specimens had not shown an adverse reaction, septicemia or death in the presence of CNC. At the point

http://dx.doi.org/10.5772/61727

4.6. Biological testing

Biological results showed 100% biocompatibility for all formulations in 16 rats. After 30 days, the specimens had not shown an adverse reaction, septicemia or death in the presence of CNC. At the point the grafts were retired, no negative influence was observed over the surface of muscles or sub-cutaneous tissues (no evidence of coagulation, fibrosis, and/or rotten or dead tissues), as can be seen in Figure 8. A further typical sign of CS in living tissues is the slight yellow color over the muscle or tissue. In a few cases rolled grafts were found, due mainly to movement of the specimen during the 30-day period. A further possible cause could be that the graft was not fixed with sutures or staples in the biological test, in order to prevent a different reaction or influence over the grafts.

Biological results showed 100% biocompatibility for all formulations in 16 rats. After 30 days, the specimens had not shown an adverse reaction, septicemia or death in the presence of CNC. At the point the grafts were retired, no negative influence was observed over the surface of muscles or sub-cutaneous tissues (no evidence of coagulation, fibrosis, and/or rotten or dead tissues), as can be seen in Figure 8. A further typical sign of CS in living tissues is the slight yellow color over the muscle or tissue. In a few cases rolled grafts were found, due mainly to movement of the specimen during the 30-day period. A further possible cause could be that the graft was not fixed with sutures or staples in the biological test, in order to prevent a different reaction or influence over the grafts.

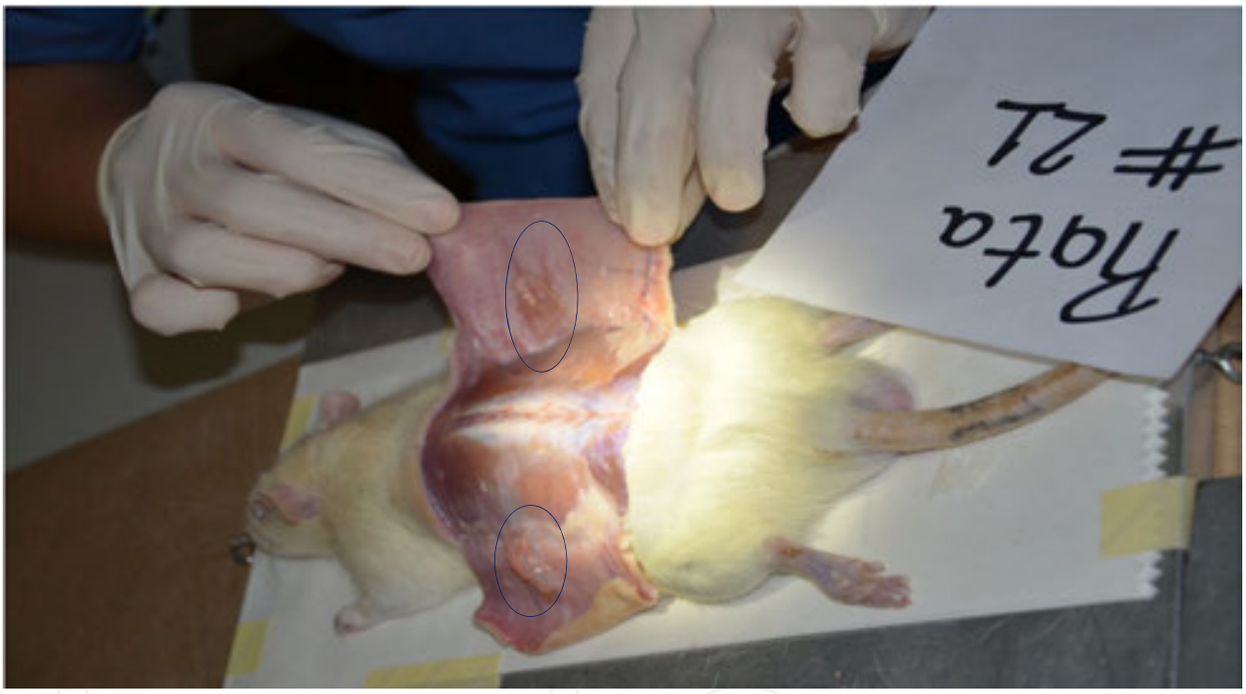

Fig. 8 Surgical stage of retiring the portions of CS + CNC (0.5 %) (circled in blue), to evaluate biocompatibility and biodegradability in the specimen.

Figure 8. Surgical stage of retiring the portions of CS + CNC (0.5 %) (circled in blue), to evaluate biocompatibility and biodegradability in the specimen.

The biodegradability values were partial but positive for all formulations, as presented in Table 3. In pure CS, the values reached between 6.21% and 8.55% in parallel. One sample had 100% biodegradability and another sample had more weight than the initial weight, suggesting the presence of new tissue as fascia and/or loose connective tissue over the graft (as presented in Figure 9), or cells or blood inside the membrane (biodegradability value: -12.89%). The CS + CNC (0.5%) had the most weight gain in their films in comparison with other formulations (-13.63%, -12.64% and -55.83% respectively). Just one sample of this group had a low biodegradability value (7.82%). For CS + CNC (1.0%) the values reached 0.71% to 21.02%. The highest values of biodegradability were shown by CS + CNC (2.0%) being 19.59% to 60.37% respectively) with just one specimen that gained weight.

The biodegradability values were partial but positive for all formulations, as presented in Table 3. In pure CS, the values reached between 6.21% and 8.55% in parallel. One sample had 100% biodegradability and another sample had more weight than the initial weight, suggesting the presence of new tissue as fascia and/or loose connective tissue over the graft (as presented in Figure 9), or cells or blood inside the membrane (biodegradability value: -12.89%). The CS + CNC (0.5%) had the most weight gain in their films in comparison with other formulations (-13.63%, -12.64% and -55.83% respectively). Just one sample of this group had a low biodegradability value (7.82%). For CS + CNC (1.0%) the values reached 0.71% to 21.02%.

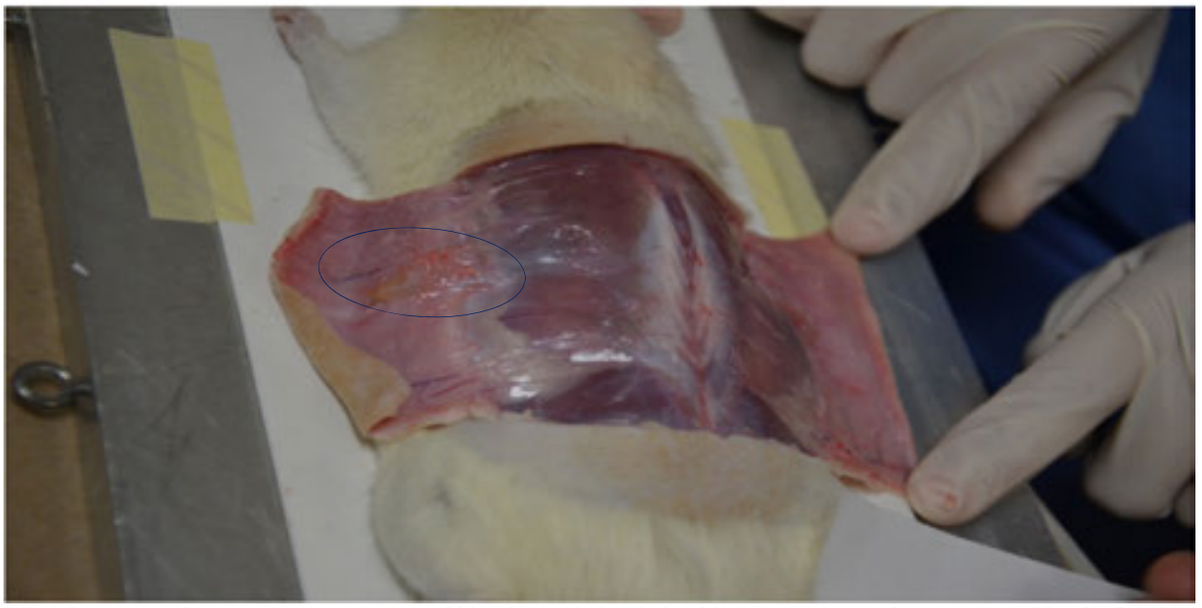

Fig. 9 Presence of loose connective tissue and blood vessels (circled in blue) formed over the portion of CS + CNC (1.0%)

Figure 9. Presence of loose connective tissue and blood vessels (circled in blue) formed over the portion of CS + CNC (1.0%)

	Biodegradability values (%)			
	Pure CS	**CS+CNC (0.5%)**	**CS+CNC (1.0%)**	**CS+CNC (2.0%)**
Specimen 1	**-12.89**	**-13.48**	8.33	19.59
Specimen 2	8.55	**-12.64**	0.71	60.37
Specimen 3	100.00	7.82	21.02	**-4.92**
Specimen 4	6.21	**-55.83**	5.52	40.52

Table 3 Biodegradability values for CS + CNC nanocomposites

	Biodegradability values (%)			
	Pure CS	CS+CNC (0.5%)	CS+CNC (1.0%)	CS+CNC (2.0%)
Specimen 1	**-12.89**	**-13.48**	8.33	19.59
Specimen 2	8.55	**-12.64**	0.71	60.37
Specimen 3	100.00	7.82	21.02	**-4.92**
Specimen 4	6.21	**-55.83**	5.52	40.52

Table 3. Biodegradability values for CS + CNC nanocomposites

Indeed, a relationship between the concentration of CNC and higher values of biodegradability can be deduced. The unstructuring effect of CNC in CS chains allows the inflow of water, cells and living fluids in the membrane. This relationship is important because it informs predictions and design of future research into different presentations of nanocomposites with higher concentrations of CNC, in order to study control of the rate of biodegradation for specific biomedical uses (depending on the part or organ in the body to be used).

Indeed, a relationship between the concentration of CNC and higher values of biodegradability can be deduced. The unstructuring effect of CNC in CS chains allows the inflow of water, cells and living fluids in the membrane. This relationship is important because it informs predictions and design of future research into different presentations of nanocomposites with higher concentrations of CNC, in order to study control of the rate of biodegradation for specific biomedical uses (depending on the part or organ in the body to be used).

The presence of loose connective tissue and fascia were evident for all formulations, as well as the formation of small blood vessels surrounding the graft. Based on the principle of time of biodegradability of new tissue, these films presented different values after 30 days. For example, CS + CNC (0.5%) showed the best results for new scaffold tissue in three formulations. In the other cases, we can estimate the total time for biodegradation to be 3–6 months (less time with higher concentrations of CNC based on these results). This could be useful in the future development of possible biomedical uses of these films.

The presence of loose connective tissue and fascia were evident for all formulations, as well as the formation of small blood vessels surrounding the graft. Based on the principle of time of biodegradability of new tissue, these films presented different values after 30 days. For example, CS + CNC (0.5%) showed the best results for new scaffold tissue in three formulations. In the other cases, we can estimate the total time for biodegradation to be 3–6 months (less time with higher concentrations of CNC based on these results). This could be useful in the future development of possible biomedical uses of these films.

Another aspect to consider with respect to biodegradation values is the type of films. In this study, non porous films were elaborated. The porosity rate and the size of pores directly affect the biodegradability of films, because they allow the easy passage of water, blood, cells and other fluids. From their condition, these films could be useful for tissue scaffolding as can be seen in Figures 10 and 11 (SEM images). A typical pattern of degradation of chitosan shown as hexagonal borders was observed in all formulations, at different stages. The formation of fascia in different stages was evident.

The presence of loose connective tissue and fascia were evident for all formulations, as well as the formation of small blood vessels surrounding the graft. Based on the principle of time of biodegradability of new tissue, these films presented different values after 30 days. For example, CS + CNC (0.5%) showed the best results for new scaffold tissue in three formulations. In the other cases, we can estimate the total time for biodegradation to be 3–6 months (less time with higher concentrations of CNC based on these results). This could be useful in the future development of possible biomedical uses of these films.

Another aspect to consider with respect to biodegradation values is the type of films. In this study, non porous films were elaborated. The porosity rate and the size of pores directly affect the biodegradability of films, because they allow the easy passage of water, blood, cells and other fluids. From their condition, these films could be useful for tissue scaffolding as can be seen in Figures 10 and 11 (SEM images). A typical pattern of degradation of chitosan shown as hexagonal borders was observed in all formulations, at different stages. The formation of fascia in different stages was evident.

Another aspect to consider with respect to biodegradation values is the type of films. In this study, non porous films were elaborated. The porosity rate and the size of pores directly affect the biodegradability of films, because they allow the easy passage of water, blood, cells and other fluids. From their condition, these films could be useful for tissue scaffolding as can be seen in Figures 10 and 11 (SEM images). A typical pattern of degradation of chitosan shown as hexagonal borders was observed in all formulations, at different stages. The formation of fascia in different stages was evident.

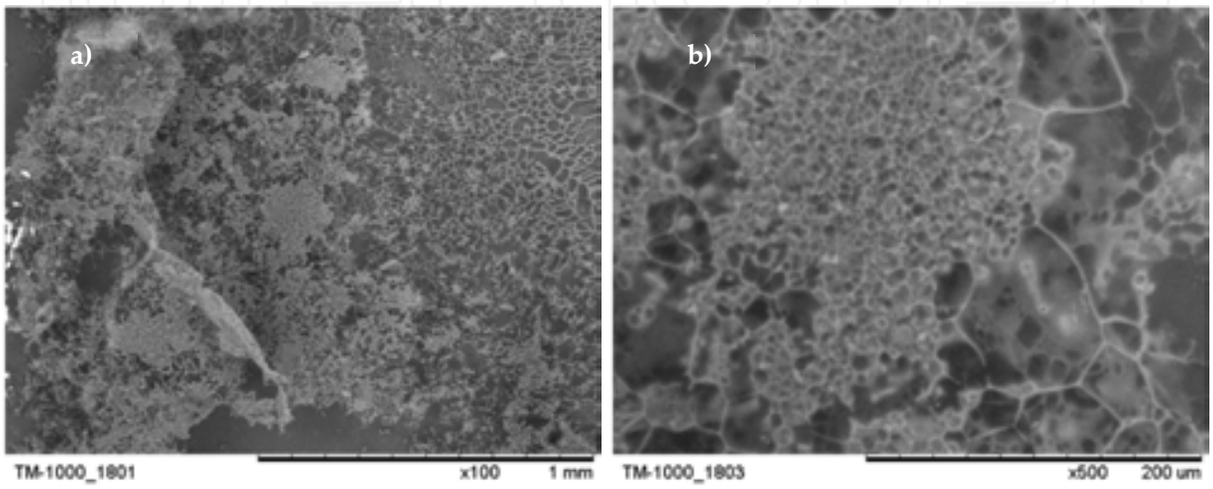

Fig 10a. Presence of loose connective tissue in CS + CNC (0.5%) films at 100x and Fig. 10b. Hexagonal pattern of chitosan degradation in CS + CNC (0.5%) at 500x.

Figure 10. a. Presence of loose connective tissue in CS + CNC (0.5%) films at 100x and Fig. b. Hexagonal pattern of chitosan degradation in CS + CNC (0.5%) at 500x.

A pattern of biodegradation of CS films is supported by the fact that the biodegradation rate of CS has a linear relationship with the Degree of Deacetylation (DD). When the DD value (from 0 to 100) is closer to 100, the material shows a slow rate of biodegradation [39]. Other aspects to consider are that CS is degraded by proteases (mainly lysozymes) that attack N-acetyl glucosamine linkages making the process faster, but these linkages have less presence in CS chains when DD values are higher. Also, in this state, lysozyme activity is low and the biodegradation rate is slow. Furthermore, CS is a semi crystalline polymer. In amorphous zones, lysozyme activity is intense and when the positive charges increase, the interactions between cells with CS are better, thereby improving biocompatibility [39].

CS scaffolds with a low Degree of Acetylation (DA) and low molecular weight have a higher rate of biodegradation. Indeed, CS scaffolds with a low DA present lower biodegradation times, smaller pores, better mechanical properties, moderate water absorption and more intense cell activity than CS scaffolds with a higher DA [40]. A pore size of between 60 and 90 microns is suitable to allow lysozymes inside the structure and to act in polymer chains.

The CS type used in this research has a DD between 75–85% and a medium molecular weight related to low biodegradation values. In CS + CNC films, the CNC had an unstructuring effect, creating spaces between CS chains, thereby allowing water (and lysozymes) access into the scaffold structure, and showing larger values of biodegradation when CNC concentration was higher.

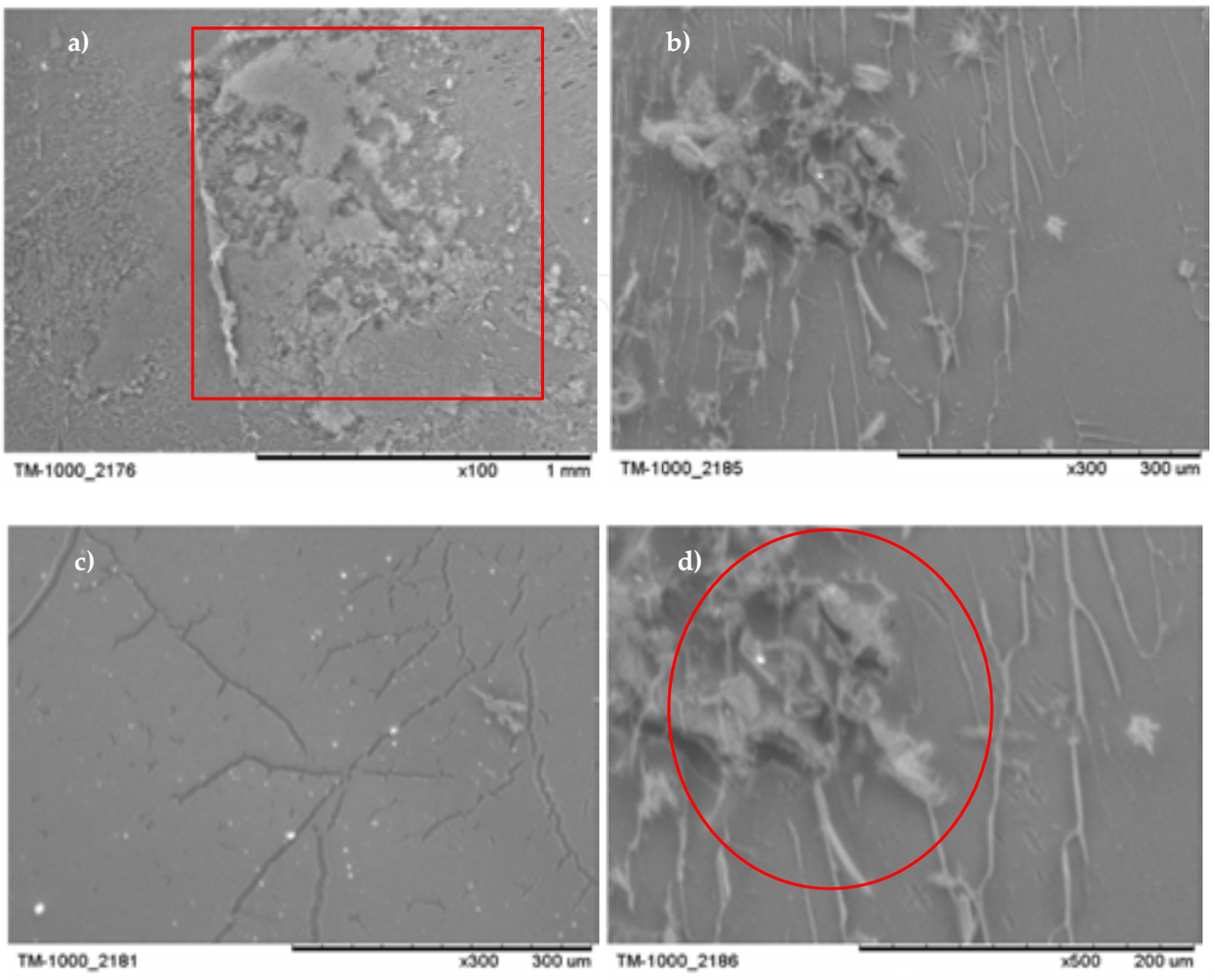

Figure 11. a. Presence of loose connective tissue (circled in red) in CS + CNC (1.0%) films at 100x and 3. 300x. Fig. 11c First steps of degradation of chitosan 11d. Presence of fascia (circled in red) in CS + CNC (1.0%) films at 500x

A pattern of biodegradation of CS films is supported by the fact that the biodegradation rate of CS has a linear relationship with the Degree of Deacetylation (DD). When the DD value (ranging from 0 to 100) is closer to 100, the material shows a slow rate of biodegradation [39]. Other aspects to consider are that CS is degraded by proteases (mainly lysozymes) that attack N-acetyl glucosamine linkages making the process faster, but these linkages have less presence in CS chains when DD values are higher. Also, in this state, lysozyme activity is low and the biodegradation rate is slow. Furthermore, CS is a semi crystalline polymer. In amorphous zones, lysozyme activity is intense and when the positive charges increase, the interactions between cells with CS are better, thereby improving biocompatibility [39].

CS scaffolds with a low Degree of Acetylation (DA) and low molecular weight have a higher rate of biodegradation. Indeed, CS scaffolds with a low DA present lower biodegradation times, smaller pores, better mechanical properties, moderate water absorption and more intense cell activity than CS scaffolds with a higher DA [40]. A pore size of between 20 and 90 µm is suitable to allow lysozymes inside the structure and to activity Mechanically, the main factor was the unstructuring effects over the chitosan chains. In biological tests, CNC show positive results for biocompatibility and biodegradability.

The CS type used in this research has a DD between 75–85% and a medium molecular weight related to low biodegradation values. In CS + CNC films, the CNC had an unstructuring effect, creating spaces between CS chains, thereby allowing water (and lysozymes) access into the scaffold structure, and showing larger values of biodegradation when CNC concentration was higher.

The attachment, morphology and proliferation of cells on CS scaffolds is highly dependent on the type of cell lines, the source and characteristics of CS, the methods of CS scaffold preparation, and the characteristics of the chitosan scaffolds. In addition, chitosan with a low molecular weight and low DA has excellent potential as a scaffolding material for a variety of tissue regeneration systems [40].

5. Conclusions

- The addition of CNC improved physical properties, increasing their capability of swelling and water capillarity. Mechanically, the main factor was the unstructuring effects over the chitosan chains. In biological tests, CNC show positive results for biocompatibility and biodegradability.

http://dx.doi.org/10.5772/61727

- CS + CNC nanocomposites showed physical, mechanical and biological properties suitable for biomedical use in recovering / wound healing, tissue scaffolding and scar prevention.
- There is a direct relationship between higher concentrations of CNC and higher values of biodegradability.
- The formation of the CS-CNC macroion complex in this study could have potential for controlled drug release taking into account other presentations of product (microspheres, nanopowders or nanoparticles).

Acknowledgements

Guillermo H. Riva, wishes to express his appreciation to the following institutions: German Exchange Students Agency (DAAD) for the scholarship and kind support during his M.Sc. Studies in Mexico; to the University of Guadalajara (UdG) for his formation as a M.Sc., for sponsorship and the financial support of this study, and Neucel Specialty Cellulose Limited (BC, Canada) for donating the alpha cellulose used in this study.

Author details

Guillermo H. Riva[1], Joaquín García-Estrada[2], Brenda Vega[2], Fernando López-Dellamary[1], María E. Hérnandez[3] and José A. Silva[1*]

*Address all correspondence to: jasilva@dmcyp.cucei.udg.mx

1 University of Guadalajara, Wood, Cellulose and Paper Research Department "Karl AugustinGrellmann" Carretera Guadalajara, Jalisco, C.P., México

2 Biomedical Research Center of Occidente (CIBO), Guadalajara, Jalisco, C.P., México

3 University of Guadalajara, Exact Sciences and Engineering Faculty, Colonia Olímpica, Guadalajara, Jalisco, C.P., México

References

[1] Habibi, Y., L. A. Lucia, Rojas, O. J. Cellulose Nanocrystals: Chemistry, Self-Assembly, and Applications. Chemical Reviews. 2010; 110(6): 3479-3500 DOI 10.1021/cr900339w

[2] Alemdar, A. and M. Sain. Biocomposites from wheat straw nanofibers: Morphology, thermal and mechanical properties. Composites Science and Technology. 2008; 68(2): 557-565. DOI:10.1016/j.compscitech.2007.05.044

[3] Sannino, A., Demitri, C., Madaghiele, M. Biodegradable Cellulose-based Hydrogels: Design and Applications. Materials. 2009; 2: 353-373. DOI:10.3390/ma2020353

[4] Shanmuganathan, K., J. R. Capadona, et al. Biomimetic mechanically adaptive nanocomposites. Progress in Polymer Science. 2010; 35(1–2): 212-222. DOI:10.1016/j.progpolymsci.2009.10.005

[5] Jonoobi, M., J. Harun, et al. Mechanical properties of cellulose nanofiber (CNF) reinforced polylactic acid (PLA) prepared by twin screw extrusion. Composites Science and Technology. 2010; 70(12): 1742-1747. DOI: 10.1016/j.compscitech.2010.07.005

[6] Oksman, K., A. P. Mathew, Bondeson, D., Kvien, I. Manufacturing process of cellulose whiskers/polylactic acid nanocomposites. Composites Science and Technology. 2006; 66(15): 2776-2784. DOI:10.1016/j.compscitech.2006.03.002

[7] Siddiqui, N. Characterization of Mechanically and Enzymatically Produced Cellulose Nanofibers from Wood Pulp. [thesis]. The Graduate School: Maine, University of Maine. 2008.

[8] Janardhnan, S., Sain, M. Targeted disruption of hydroxyl chemistry and crystallinity in natural fibers for the isolation of cellulose nano-fibers via enzymatic treatment. BioResources. 2011; 6(2): 1242-1250. DOI: 10.15376/biores.6.2.1242-1250

[9] Jonoobi, M., Harun, J., Mathew, A.P., Hussein, M.Z., Oksman, K. Preparation of cellulose nanofibers with hydrophobic surface characteristics. Cellulose. 2010; 17: 299-307. DOI 10.1007/s10570-009-9387-9

[10] Kalia, S., A. Dufresne, Cherian, B., Keith, B. S., Avérous, L., Njuguna, J. Cellulose-Based Bio- and Nanocomposites: A Review. International Journal of Polymer Science. 2011, (Article ID 837875): 35. DOI:10.1155/2011/837875

[11] Shelma R., Willi Paul and Sharma C.P. Chitin Nanofibre reinforced Chitosan Films for Wound Healing Application. Trends Biomater. Artif. Organs. 2008; 22(2): 111-115

[12] Hui, J., Yuanyuan, J., Jiao, W., Yuan, H., Yuan, Z., Shiru, J. Potentiality of Bacterial Cellulose as the Scaffold of Tissue Engineering of Cornea. 2nd International Conference on Biomedical Engineering and Informatics (BMEI 2009). DOI 10.1109/BMEI. 2009.5305657

[13] Schumann, D., J. Wippermann, *et al.* Artificial vascular implants from bacterial cellulose: preliminary results of small arterial substitutes. Cellulose. 2009; 16(5): 877-885. DOI 10.1007/s10570-008-9264-y

[14] Amorim, W. L., Costa, H. O., Coehlo de S., F., Germanos de C., M., da Silva, L. Experimental study of the tissue reaction caused by the presence of cellulose produced by Acetobacter xylinum. Brazilian Journal of Otorhinolaringology. 2009; 75(2): 200-207. DOI 10.1590/S0034-72992009000200008

[15] de Mesquita, J. P., Donnici, C. L., Pereira, F. V. Biobased Nanocomposites from Layer-by-Layer Assembly of Cellulose Nanowhiskers with Chitosan. Biomacromolecules. 2010; 11(2): 473-480. DOI 10.1021/bm9011985

[16] Darder, M., López-Blanco, M., Aranda, P., Aznar, A.J., Bravo, J., Ruiz-Hitzky, E. Microfibrous chitosan-sepiolite nanocomposites. Chemical Materials. 2006; 18: 1602-1610. DOI 10.1021/cm0523642

[17] Gupta, K. C. and M. N. V. R. Kumar. Structural changes and release characteristics of crosslinked chitosan blends in response to solution pH. Journal of Macromolecular Science, Part A. 1999; 36(5-6):827-841.DOI:10.1016/S1381-5148(00)00038-9

[18] [18} Madihally, S. V. and H. W. T. Matthew. Porous chitosan scaffolds for tissue engineering. Biomaterials. 1999; 20(12): 1133-1142. DOI:10.1016/S0142-9612(99)00011-3

[19] Azeredo, H. M., L. H. Mattoso, Avena-Bustillos, R. Ceotto, G., Munford, M., Wood, D., Mc Hugh, T. Nanocellulose reinforced chitosan composite films as affected by nanofiller loading and plasticizer content. Journal of Food Science. 2010; 75(1): N1-7. DOI: 10.1111/j.1750-3841.2009.01386.x

[20] Jeon, Y. J., Kamil, J.Y.V.A., Shahidi, F. Chitosan as an edible invisible film for quality preservation of herring and Atlantic cod. Journal of Agriculture and Food Chemistry. 2002; 50: 5167–5178. DOI: 10.1021/jf011693l

[21] Bangyekan, C., D. Aht-Ong, Aht-Ong, D., Srikulkit, K. Preparation and properties evaluation of chitosan-coated cassava starch films. Carbohydrate Polymers. 2006; 63(1): 61-71. DOI:10.1016/j.carbpol.2005.07.032

[22] Durango, A. M., Soares, N.F.F., Andrade, N.J. Microbiological evaluation of an edible antimicrobial coating on minimally processed carrots. Food Control. 2006; 17: 336-341. DOI:10.1016/j.foodcont.2004.10.024

[23] Campaniello, D., Bevilacqua, A., Sinigaglia, M., Corbo, M. R. Chitosan: antimicrobial activity and potential applications for preserving minimally processed strawberries. Food Microbiology. 2008; 25(8): 992-1000. DOI:10.1016/j.fm.2008.06.009

[24] Nisperos-Carriedo. Edible coatings and films based on polysaccharides. Edible coatings and films to improve food quality. 1994. J. M. Krochta, Baldwin, Nisperos-Carriedo. Lancaster, U. K., Technomic. 305-335.

[25] Suyatma, N. E., Copinet, A., Coma, V., Tighzert, L. Mechanical and barrier properties of biodegradable films made from chitosan and poly(lactic acid) blends. Journal of Polymer Environment. 2004; 12: 1-6. DOI: 10.1023/B:JOOE.0000003121.12800.4e

[26] Suyatma, N. E., Tighzert, L., Copinet, A. Effects of hydrophilic plasticizers on mechanical, thermal, and surface properties of chitosan films. Journal of Agriculture and Food Chemistry. 2005; 53(10): 3950-3957. DOI 10.1021/jf048790+

[27] Di Gioia, L., Guilbert, S. Corn Protein-based Thermoplastic Resins: Effect of some Polar and Amphiphilic Plasticizers. Journal of Agriculture and Food Chemistry. 1999; 47: 1254-1261. DOI: 10.1021/jf980976j

[28] Ludueña, L. N., Alvarez, V.A., Vasquez, A. Prossesing and microstructure of PCL/clay nanocomposites. Materials Science and Engineering A. 2007; 460-461: 121-129. DOI:10.1016/j.msea.2007.01.104

[29] Sorrentino, A., Gorrasi, G., Vittoria, V. Potential perspectives of bionanocomposites for food packaging applications. Trends in Food Science & Technology. 2007; 18(2): 84-95. DOI:10.1016/j.tifs.2006.09.004

[30] Vaia, R. A., Wagner, H.D. Framework for nanocomposites. Materials Today. 2004; 7: 32-37. DOI:10.1016/S1369-7021(04)00506-1

[31] Park, T.-J., Y. Jung, Choi, S. W., Park, H., Kim, H., Kim, E., Lee, S. H., Kim, J. H. Native chitosan/cellulose composite fibers from an ionic liquid via electrospinning. Macromolecular Research. 2011; 19(3): 213-215. DOI:10.1007/s13233-011-0315-0

[32] Jacobs, V., Patanaik, A and Anandjiwala, R.D. Electrospun chitosan nanofibre membranes for antimicrobial application: role of electrospinning processing parameters. European Cells and Materials. 2010; Vol. 19. Suppl. 1, pp 4. ISSN 1473-2262.

[33] Macías, H. Quitosana como andamiaje celular en regeneración de membrana timpánica en conejo Nueva Zelanda (timpanoplastía experimental tipo I) [thesis]. Departamento de Neurociencias. Guadalajara, Universidad de Guadalajara 2010.

[34] ASTM D 587 - 98 Standard Test Method for Swelling and Water Retention (1998)

[35] Fernandes, S., Freire, C., Silvestre, A., Neto, C. P., Gandini, A., Berglund, L., Salmén, L. Transparent chitosan films reinforced with a high content of nanofibrillated cellulose. Carbohydrate Polymers. 2010; 81: 394-401. DOI:10.1016/j.carbpol.2010.02.037

[36] Khan, A., Khan, R. A., Salmieri, S., Le Tien, C., Riedl, B., Bouchard, J., Chauve, G., Tan, V., Kamal, M. R., Lacroix, M. Mechanical and barrier properties of nanocrystalline cellulose reinforced chitosan based nanocomposite films. Carbohydrate Polymers. 2012; 90: 1601– 1608. DOI:10.1016/j.carbpol.2012.07.037

[37] Wang, H., Roman, M. Formation and properties of chitosan-cellulose nanocrystal polyelectrolite-macroion complexes for drug delivery applications. Biomacromolecules. 2011; 12: 1585-1593. DOI: 10.1021/bm101584c

[38] Mathew, A. P., Laborie, M.P., Oksman, K. Cross-linked chitosan/chitin crystal nanocomposites with improved permeation selectivity and pH stability. Biomacromolecules. 2009; 10(6): 1627-1632. DOI: 10.1021/bm9002199

[39] Croisier, F., Jerome, C. Chitosan based biomaterials for Tissue Engineering. European Polymer Journal. 2013; (49) 780 – 792. DOI: 10.1016/j.eurpolymj.2012.12.009.

[40] Han, T., Nwe, N., Furuike, T., Tokura, S., Tamura, H. Methods of N – acetylated chitosan scaffolds and it's *in vitro* biodegradation by lysozyme. J. Biomedical Science and Engineering, 2012; (5): 15-23. DOI: 10.4236/jbise.2012.51003.